https://doi.org/10.5564/mgs.v29i58.3448

Mongolian Geoscientist

Original Article

Petro-chemical characterization and depositional setting of a Late Permian high ash coal deposit, Central Mongolia

Per Michaelsen[1]*, Batbold Demberelsuren[2]

[1]Geoscience Center, School of Geology and Mining Engineering, Mongolian University of Science and Technology, Ulaanbaatar, 14191, Mongolia
[2]Ukhaakhudag coal mine, Branch of Energy Resource LLC, Tsogttsetsii, 46000, Umnugovi, Mongolia

*Corresponding author: perm@must.edu.mn, ORCID: 0000-0003-4075-8943

ARTICLE INFO

Article history:

Received: 04 January, 2024
Revised: 19 May, 2024
Accepted: 24 May, 2024

ABSTRACT

Pan global Permian coal measures are unique in the evolution of the Earth, not matched in any period before or since. Middle and late Permian coal-bearing strata are widely distributed in Mongolia. In particular, a large concentration of transtensive coal-bearing sub-basins is located in southern Mongolia, some of which are well documented. However, the late Permian coal measures developed along the shores of the Mongol-Transbaikalian Seaway in central Mongolia, the focus of this contribution, has received very limited attention. This study focuses on the c. 420 m thick coal-bearing middle part of a c. 2,600 m thick Permo-Triassic succession in the Bayanjargalan district. The study draws on data from 38 drillholes, 3 km of trenches, mapping, petrological analysis of sandstone samples, analysis of macroflora, fauna and trace fossils, 82 coal quality samples as well as washability and ash XRD analysis from a 3t coal bulk sample. The unstable and wedge-shaped architecture of the coal seams strongly suggest a syn-tectonic influence on their development. Paleoclimatic indicators suggest the peat mire ecosystem developed during relatively cold - temperate climatic conditions. Peat-forming plants such as *Cordaites*, *Rufloria* and *Koretrophyllites* probably benefited from moist air currents along the seaway. Plant-arthropod interactions are reported from two sites, in particular DT228 and DT246 oviposition lesions, the latter being almost twice the size of a previous report from North America. Results from 82 proximate analyses returned consistent very high ash yields of 46.95% (db) and 43.45% (adb) from the 3t bulk sample, which are unusual for Permian coals in Mongolia.

Keywords: Mongol-Transbaikalian Seaway, coal measures, coal quality, facies analysis, plant-arthropod interactions

INTRODUCTION

Tectonic, eustatic, climatic, and auto-sedimentary processes are normally considered to be the major influences controlling sediment distribution, stacking patterns, and seam splitting (Weisenfluh and Ferm 1984; Ferm and Staub 1984; Surlyk et al. 1995; Michaelsen et al., 2000). This contribution documents and interprets a c. 420 m thick late Permian very high ash coal deposit which appears to be mainly influenced by syn-tectonic deposition.

Extensive field work across southern and central Mongolia for numerous international and Mongolian coal and coal bed methane (CBM) exploration companies during the past two decades by the senior author, shows that there is every reason to believe that during late Permian times inertia-driven transtensive reactivation

of primordial fracture zones gave rise to the development of a sequence of related but disconnected fault-bounded sub-basins; some of these became the locus of substantial peat accumulation that evolved into economically important coal deposits (Michaelsen and Storetvedt, 2023, 2024).

The vast majority of the Permian sub-basins sporadically outcrop north of the Chinese border from c. 95° -109°E with the main concentration in the South Gobi region. Global wrench tectonics, a relatively new global tectonic theory based on the inertia principle for the rotating Earth, in conjunction with the ubiquitous orthogonal fracture/fault system (Storetvedt, 2003), best explains the sub-basins scattered spatial distribution associated with wrench faults.

Michaelsen and Storetvedt (2024) noted that syn-tectonic sedimentation continued across the Permo-Triassic boundary within numerous sub-basins, in central and southern Mongolia such as Bayanjargalan, Navtgar Uul, Yangir, Khuts Uul, Erdenebulag, Bayan Ovoo west, Tsant Uul, Bulag Suuj and Noyon, recording a distinct climatic change from humid cold-temperate coal-forming environments, to relatively arid desolate conditions in the early Triassic (ie. characterized by carbonate nodules, barren greenish mudstone and alluvial fan deposits).

The Permian coal deposits in southern Mongolia have received some interest over the years (Jargal et al., 1990; Orolmaa et al., 1999; Johnson et al., 2007; Erdenetsogt et al., 2009; Demberelsuren et al., 2021; Cai et al., 2022; Demberelsuren et al., 2023; Michaelsen and Storetvedt, 2024). However, the late Permian coal measures preserved in the Bayanjargalan area in central Mongolia, c. 135 km southeast of Ulaanbaatar (Fig. 1), have only received limited attention (Erkhembaatar et al., 1995; Michaelsen, 2016; Michaelsen and Storetvedt, 2023), with this contribution building and expanding on the previous work based on new data and observations Rapid facies changes, the unstable nature and wedge shaped architecture of the coal seams combined with the consistent very high ash content, observed in the coal measures at Bayanjargalan strongly suggest syn-tectonic processes exerted a fundamental control on the depositional dynamics and facies architecture at district scale.

Climatic indicators within the coal measures include well developed growth rings in fossilized wood and a rare cluster of glendonites at the base, indicat cold to temperate climatic conditions during deposition. Recent detailed growth ring analysis on fossilized wood obtained from late Permian coal measures within the Tsagaan Tolgoi sub-basin in South Gobi by Cai et al. (2022), suggested relatively short growing seasons. Further, Cai et al. (2022) discovered a

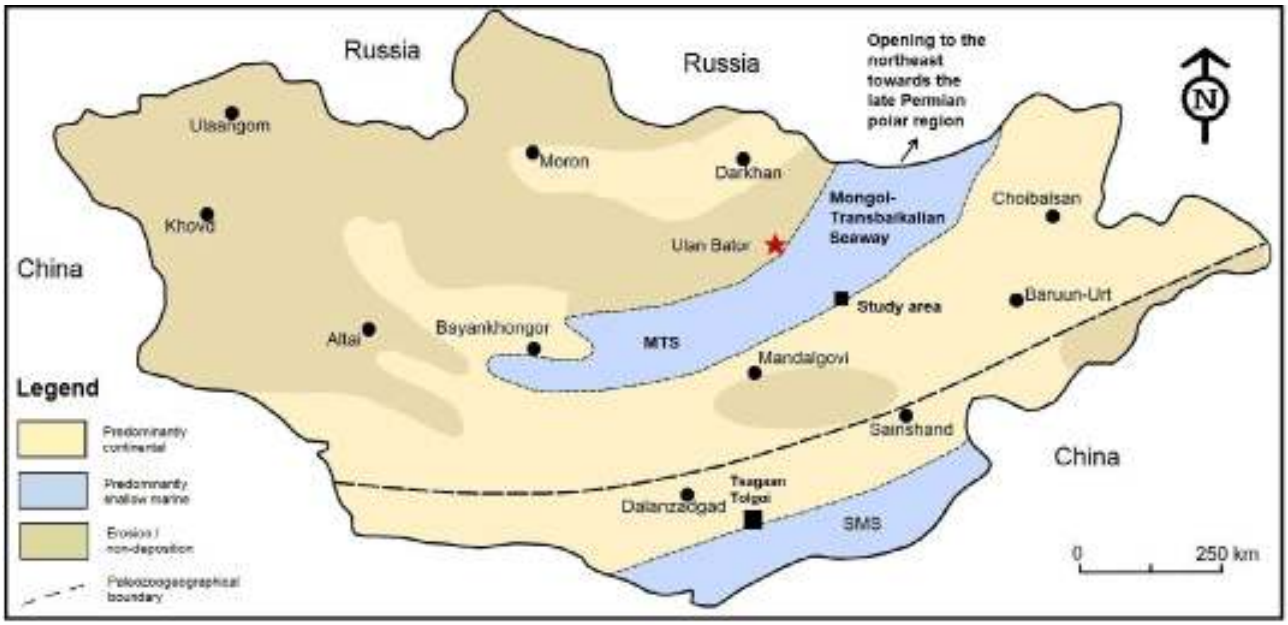

Fig. 1. Generalized spatial distribution map of Permian sedimentary strata in Mongolia showing locations of the study area and the Tsagaan Tolgoi sub-basin (modified from Manankov et al., 2006).

growth interruption, probably recording an early spring cooling event in a temperate climate. The results from this study coupled with the recent results from Cai et al. (2022) indicate relatively cold climatic conditions prevailed in both central and southern Mongolia during late Permian times. Furthermore, extensive field work in the Tsagaan Tolgoi sub-basin (Fig. 1) has revealed a number of important similarities with the current study area which are discussed in this contribution.

GEOLOGICAL SETTING

The focus of this district scale study is a 2,223 hectares area located in central Mongolia (Fig. 2). The study area is situated in the southern part of a c. 26 km long northeast trending, V shaped fault-bounded sub-basin in the Bayanjargalan

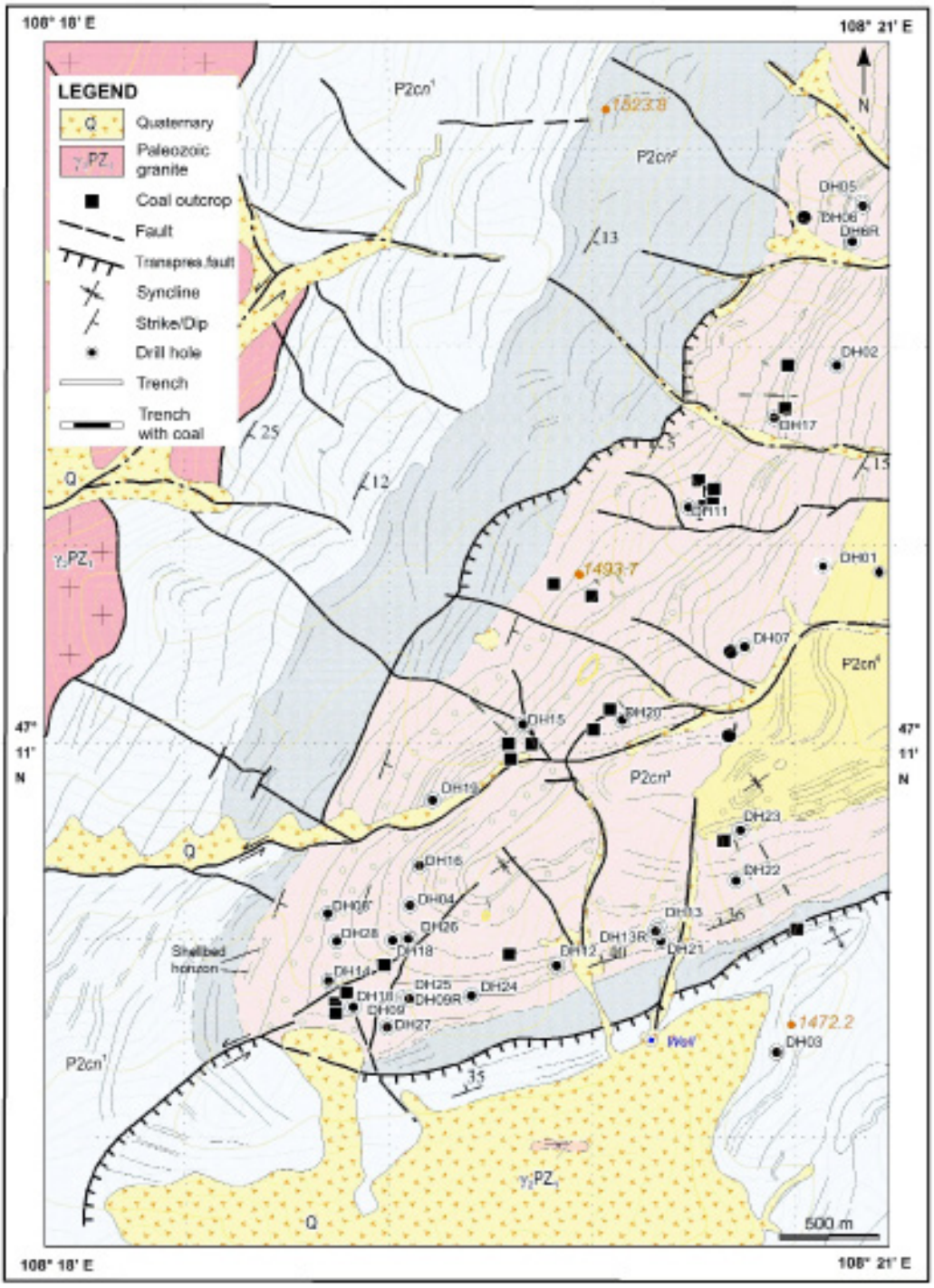

Fig. 2. Geology map of the study area showing location of drill holes, strike/dip measurements, topography, bedding, faults, syncline/anticline, stratigraphic units, coal outcrops, shell bed and trenches with coal intersections (modified from Michaelsen, 2016).

area. The sub-basin developed along the southern margin of the Mongol-Transbaikalian Seaway (MTS, Fig. 1), formerly known as the Khangai-Khentei Geosyncline (Manankov 1999 and references therein).

The MTS is widely regarded as the southern extension of the Permian Mongol-Transbaikalian biogeographical province of the Boreal zoogeographical realm (Manankov 1998, 1999, 2012). The Permian succession of the MTS is sporadically exposed over a length of c. 900 km and a maximum width of c. 150 km, with the most extensive outcrops west of Delgertsogt in the western sector. The Mongol-Transbaikalian Seaway had its opening to the northeast, towards the polar region of the time (Biakov et al., 2013), and thus may reinforce the possibility of a relatively cool late Permian climate in northeastern Mongolia (Michaelsen and Storetvedt, 2023, 2024). Minor early Tatarian limestone beds are sporadically exposed in the Binder district (48°35'N/110°33E), which clearly argue for periods with warmer climatic periods during that stage. Somewhat similar findings were recently reported in a detailed study by Fielding et al. (2022) from NE Australia where the Lopingian (257-251.9 Ma) succession were investigated and several major late Permian palaeoenvironmental changes were noted by the authors.

The MTS experienced several deep regressive events during the mid and late Permian as indicated by the work of Manankov as well as data collected during recent field work by the senior author around Adaatsag, Delgertsogt, Tsenkhermandal, Jargaltkhan, Bayan, Bayantsagaan, Bayanjargalan, Binder and other localities. Recent results from Michaelsen and Storetvedt (2023, 2024) shows that at the end of the Permian the relatively shallow epicontinental seaway underwent a dramatic drainage, marking the most severe biological disaster in Earth history (Hansen et al., 2000; Michaelsen and Henderson, 2000b; Michaelsen et al., 2000; Rampino et al., 2000; Yin et al., 2001; Huang et al., 2011; Brand et al., 2012; Retallack, 2013; Burgess et al., 2014). This prolonged degassing event which was possibly linked to upper crustal loss to the mantle in the Siberian Traps region (Storetvedt and Michaelsen, 2024), led to the most dramatic biological disaster in Earth history (Michaelsen, 2002).

Regional mapping work by a Russian-Mongolian team during 1947 headed by Homizuri and Bolkhovitina, included the Bayanjargalan study area, and established a late Permian age based on analysis of marine fossils in the middle part of the c. 2,600 m thick sedimentary package (Fig. 3). Subsequently the late Permian age was reconfirmed in 1965 by another Russian-Mongolian mapping expedition, headed by Khapov, based on plant fossils in the lower-middle part of the succession. The significant sedimentary fill was subsequently subdivided into five late Permian stratigraphic units of the Tsenkher Gol Formation by Erkhembaatar et al. (1995) and modified by Michaelsen (2016). It is noted that subsequent to the work by Erkhembaatar et al. (1995) the Mongolian Commission on Stratigraphy accepted the international Permian system with three series in 2016. Nonetheless, four of the five original Permian stratigraphic sub-division by Erkhembaatar et al. (1995; ie. P_2cn_{1-4}) is upheld for now while undergoing stratigraphic review. The sole focus of this contribution is the c. 420

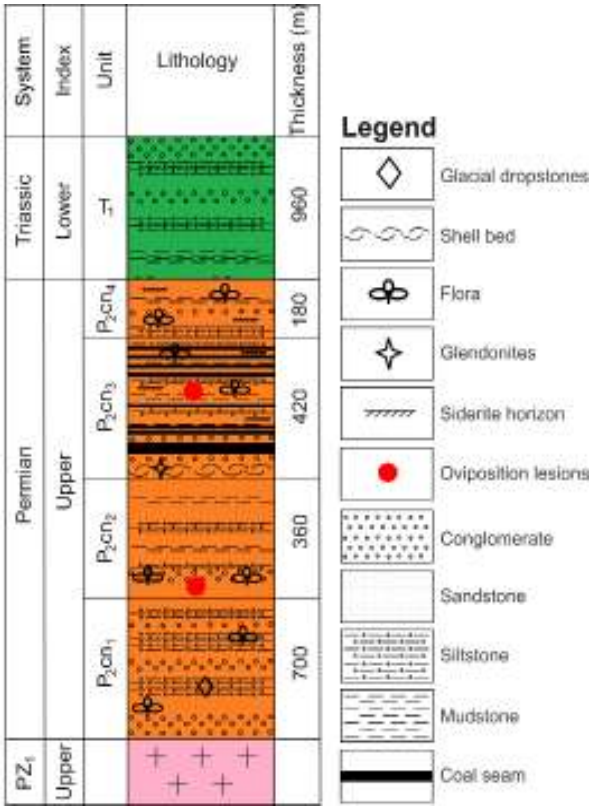

Fig. 3. Schematic stratigraphic framework of the Permo-Triassic Bayanjargalan sub-basin.

m thick middle coal-bearing stratigraphic unit (Fig. 3, Table 1).

The middle coal-bearing unit (P_2cn_3) conformably overly c. 1,060 m of predominantly shallow marine sandstone beds, punctuated by marked regressive events where plants relatively briefly colonized the exposed seaway landscape (Table 1). A sample from a sea-level lowstand outcrop of this stratigraphic interval, revealed a fertile spike of a *taeniopterid*, the morphology did not develop until earliest late Permian and continued into the Triassic (Rigby, pers. com).

The coal measures are in turn conformably overlain by c. 180 m of predominantly shallow marine deposits with some sections of this transitional unit being highly bioturbated by an assemblage of *Thalassinoides, Skolithos* and *Planolites* ichno fossils (Table 1, Fig. 3). Furthermore, shell fragments were recently discovered and documented by the senior author within siderite nodules proximal northeast of the study area.

The coal measures are made up of a marine shell bed at the base (Fig. 3), polymictic conglomerate, sandstone, siltstone, carbonaceous mudstone and up to eight high ash coal seams (Michaelsen, 2016). The rapid thickness variations and unstable nature of the coal seams strongly suggest a syn-tectonic influence on their development, which appears to be common within middle-late Permian coal measures in Mongolia based on extensive field work observations.

The peat mire ecosystem is considered to have developed during boreal to temperate climatic conditions along the shores of the MTS. The seaway was likely frozen during the dark cold winter months, and benefited from moist air currents along the seaway during the relatively short summer months, with Diessel (1992) noting that short nights favor steady plant growth.

The V-shaped sub-basin at Bayanjargalan taper out towards the southwest and has a maximum width of c. 12 km. The c. 2,600 m thick sedimentary fill is considered here to be one of the most significant Permo-Triassic successions in Mongolia. The sub-basin was considered by Michaelsen and Storetvedt (2023) to have developed as a result of reactivation of deep primordial wrench faults, with the sedimentary fill warped into a relatively gently dipping asymmetrical syncline as a result of wrench tectonic transpression, possibly during late Jurassic times.

A number of predominantly NE oriented sinistral wrench faults, with horizontal displacement of up to 300 m, occur within the study area (Fig. 2). The vertical component of the wrench faults appears to have played an important role in peat mire development with localized thickening of peat proximal to these structures (ie. on the

Table 1. General overview of the five informal Permo-Triassic stratigraphic units and their main attributes.

Chronology	Lithostratigraphy		Approximate Thickness (m)	Fossils	Paleoclimatic Indicators	Depositional Systems	Environmental Conditions
	Formation	Sub-Group					
Early Triassic		T^1	960	Barren	Barren greenish mudstones	Alluvial fan Fluvial	Relatively arid desolate conditions
Late Permian	Tsenkher Gol	$P_2 cn^4$	180	Abundant *Thalassinoides*, *Skolithos* and *Planolites* ichno fossils in places. Shell fragments in siderite nodules	Siderite nodules	Predominantly shallow marine	Common base-level changes
		$P_2 cn^3$	420	*Koretrophyllites* macroflora. Shellbed with cold resistant taxodont bivalves, archaeogastropods and Conulariid fragments. *Ophiomorpha cf. nodosa. Planolites.* Petrified wood. Oviposition lesions	Glendonites Petrified wood with strongly developed annual growth rings. Siderite horizons	Cold resistant peat mire ecosystem developed on coastal plain, inter-fingering with near shore depositional system	Cold climate with high-wind regime. High frequency base-level changes. Major sequence boundary developed at base
		$P_2 cn^2$	360	*Taeniopteris* sp. macroflora Petrified wood with oviposition lesions	Petrified wood with strongly developed annual growth rings	Predominantly shallow marine interrupted by noticiable regressive events	Boreal. Common base-level changes
		$P_2 cn^1$	700	*Rufloria* macroflora. Abundant ichno fossils in places	Glacial erratics		

downthrown side characterized by accelerated subsidence).

The study area is characterized by close spaced orthogonal jointing, resulting in very fragmented and sporadic outcrops. In this context this contribution is primarily based on sub-surface data from 38 drillholes and 3,000 m of shallow trenches.

MATERIALS AND METHODS

This study is part of an ongoing Permo-Triassic research project which encompasses the entire Mongol-Transbaikalian Seaway and the southern Mongolian coal-bearing sub-basins. The study has drawn on a relatively new database compiled in the context of district-scale exploration work targeting high energy coal seams as well as more recent field work. The results of the exploration work (including all coal quality data) were continuously disclosed to the Australian Stock Exchange by Newera Resources, and as such in the public domain. The database consists of 38 drillholes (ie. including three re-drills) totaling 2,703.2 m in composite length (Table 3, Fig. 2) and almost 3,000 m of shallow trenches. The present study is based on months of field work from 2012 to 2023, including mapping, detailed lithological logging of drill core, photo documentation, sampling and geophysical logging of 38 drill holes. The exploration drilling mainly targeted the thick basal coal seam horizon along strike. The average hole depth is 71.14 m with the deepest corehole drilled to a depth of 300 m (ie. DH02, Fig. 2). Event signatures, lithofacies contacts, sandstone attributes, biogenic features, sedimentary structures and coal characteristics were given special attention during the logging program. Trace fossil intensity is based on the bioturbation intensity index (BII); as none 0, low 1-2, moderate 3, high 4 and intense 5-6 (Bann and Fielding, 2004). All thickness referred to here are apparent thickness. Furthermore, a total of 82 coal core samples were analyzed for proximate, coking properties, relative density and CV.

A 3t bulk sample of fresh coal derived from an inclined trial shaft in the southern area of the coal measures was used for washability testing, initially by Sedgeman with subsequent testing by Bureau Veritas (BV) Mongolia. Petrological analysis of selected sandstone samples were conducted at Mongolian University of Science and Technology. This study has also drawn on previous work by Russian and Mongolian regional surveys (Erhembaatar et al., 1995) as well as recent field work north and south of the study area from 2018-2023. Numerous world-

Table 2. Summary of lithofacies characteristics from the late Permian coal measures (P_2 cn_3)

Facies Association	Lithology	Sedimentary Structures	Geometry	Facies Bounding Surfaces	Fossils	Depositional System
1	Predominantly medium-grained sandstone (pebbly in places)	Thin sets of trough-cross stratification and planar bedding	Ribbons up to 35.1m thick	Sharp, irregular, erosional	Fragmented petrified wood	Non-perennial flashy fluvial channels
2	Siltstone, sandstone and carbonaceous mudstone	Planar bedding and ripple lamination	Wedges and lobes proximal-distal to FA1	Sharp, planar, non-erosional	*Koretrophyllites*	Levee / overbank to floodbasin
3	High ash coal	Planar lamination	Unstable sheets up to 19.45 m thick x +10 km	Sharp, planar, non-erosional		Wet peat mire Moderately high flooding
4	Predominantly elongate clast-supported, extra-formational conglomerate	Planar bedding	Extensive (c. 20 km) ribbons up to 3.1 m thick	Sharp, irregular, erosional		Gravelly beachface
5	Interbedded sandstone and carbonaceous siltstone/ mudstone	Disturbed, planar, wavy and lensen bedding. Scour and fill structures	Relatively thin sheets	Sharp, planar, non-erosional	Abundant ichno fossils *(Planolites, Thalassinoides and Skolithos)*	Tidal flat
6	Well sorted very fine-grained sandstone and siltstone. Crystal clusters of *Glendolites*	Horizontal bedding and lower flow regime symmetrical wave ripples	Extensive (+11 km) sheets	Sharp, irregular, erosional	Shellbed with cold resistant taxodont bivalves, archaeogastropods and *Conulariida* fragments. *Ophiomorpha cf. nodosa.*	Upper to lower shore face

class experts assisted with identifying the late Permian flora, fauna, trace fossils and plant-insect interactions (see Acknowledgements).

RESULTS

Facies analysis of the coal-bearing strata

The results from extensive field work shows the late Permian coal measures are characterized by six facies associations (FA) which were initially documented by Michaelsen (2016) and later briefly noted by Michaelsen and Storetvedt (2023) in table format. The six facies associations have been reviewed based on results from recent field work and described in more detail in the following and summarized in Table 2. Given the relatively poor natural exposures most of the FA data was obtained from the 38 drill holes (Table 3) and c. 3,000 m of shallow trenches.

Table 3. Overview of the drill hole database with location, hole type, total depth and net coal thickness. Projection: UTM Zone 49, Northern Hemisphere (WGS 84)

Drill Hole #	Hole Type	UTM (Northing)	UTM (Easting)	Total Depth (m)	Total Net Coal	RL (m)
DH01	Core	299255	5229880	114	0.1	1,406
DH02	Core	299189	5230915	300	14.7	1,428
DH03	Core	298895	5227435	103	0	1,462
DH04	Core	297102	5228183	164.5	6.67	1,442
DH05	Core	299313	5231721	39	2.2	1,416
DH06	Core	299310	5231740	40	1.8	1,439
DH6R	Core	299263	5231545	50	7.1	1,405
DH07	Core	298739	5229489	57.2	0	1,438
DH08	Core	296690	5228137	46	0.24	1,458
DH09	Core	297053	5227705	40	12	1,418
DH09R	Core	297069	5227712	56	19.45	1,421
DH10	Core	296821	5227648	54.5	0.57	1,413
DH11	Core	298461	5230197	32.5	7	1,455
DH12	Core	297818	5227876	42.5	0	1,424
DH13	Core	298295	5228056	8	0	1,416
DH13R	Core	298311	5228076	46	6.4	1,413
DH14	Core	296697	5227802	44	12.8	1,418
DH15	Core	297650	5229100	35	2.5	1,435
DH16	Core	297147	5228384	30	2	1,455
DH17	Core	298877	5230651	50	7.5	1,419
DH18	PCD	297016	5228007	62	2.7	1,431
DH19	PCD	297205	5228718	38	4.3	1,439
DH20	PCD	298135	5229116	26	2.8	1,450
DH21	PCD	298336	5227995	23	0.3	1,416
DH22	PCD	298695	5228305	17	2	1,441
DH23	PCD	298719	5228564	28	1.6	1,430
DH24	PCD	297395	5227726	44	3.63	1,430
DH25	Core	297092	5227711	100	21.98	1,422
DH26	Core	297089	5228013	150	18.55	1,427
DH27	Core	296984	5227569	160	18.34	1,410
DH28	Core	296735	5228000	110	5.77	1,429
DH29	PCD	297720	5231800	150	0	1,510
DH30	PCD	299238	5231939	50	6.1	1,426
DH31	PCD	299324	5231787	50	14.5	1,420
DH32	PCD	299081	5231623	58	7.6	1,404
DH33	PCD	299246	5231313	50	7.2	1,410
DH34	PCD	297520	5228525	200	8.4	1,432
DH35	PCD	299326	5231790	35	5.6	1,420

Facies 1: Fluvial channels

Facies 1 is dominated by light grey fine to coarse-grained pebbly sandstone (Fig. 4), with subordinate medium grey siltstone and clast-supported conglomerate. Extra-formational conglomerate lag deposits are up to 18.9 cm thick with individual clasts up to 3.6 cm in length. Bedding thickness varies from thin to thick, generally medium with common fining-upward cycles (Fig. 4). The sandstone dominated units are up to 35.1 m thick (ie. intersected in drill hole DH02, Fig. 2). Microscopic modal analysis of sandstone samples from these facies shows that they are quartz and feldspar-rich characterized by textural immaturity, with individual grains being predominantly angular to sub-angular. Rare outcrops of Facies 1 show well developed trough-cross stratification with sets up to 21 cm. Finely disseminated to coarser organic debris are commonly preserved along bedding planes.

Fig. 4. Rare exposure of FA 1 showing pebbly sandstone (ie. active channel fill) with thin fining upward sequences characterized by abrupt contacts indicating short flashy discharge periods. Similar characteristics were noted in numerous late Permian sub-basins in South Gobi.

With regards to facies stacking patterns the base of the sandstone bodies are positioned at least 0.3 m above coal horizons (FA 3). Paleocurrent measurements obtained from a Facies 1 outcrop indicate axial (ie. NE-SW) sediment dispersal (Fig. 5). Fossil wood fragments documented from Facies 1 outcrops shows very well-developed growth rings (Fig. 6).

Facies 1 is interpreted as representing the fill of mixed-load fluvial channels on the lower coastal plain. The history of channel infilling and the style of fluvial channel systems are commonly complex and difficult to decipher (see among others Bridge 1993; Smith 1970; Miall 1996; Michaelsen et al., 2000). Facies stacking patterns and bounding surfaces indicate relatively rapid aggradation during high stand systems tract times (Li and Zhang, 2017 and references therein). Given the typical gradient on the lower coastal plain is generally in the order of 1-10 feet/mile (0.3-3 m/1.6 km) it would be reasonable to assume a sinuosity index >1.5 (Miall, 1996; Wu et al., 2023) Unfortunately, the width/thickness ratios and architecture of these meandering lowland channels is unknown given the poor surface exposures coupled with the sporadic and low density drill hole coverage (Fig. 2). Nonetheless, the significant thickness of the sandstone bodies in places such as in drill hole DH02, indicate the channels were constrained for prolonged periods of time,

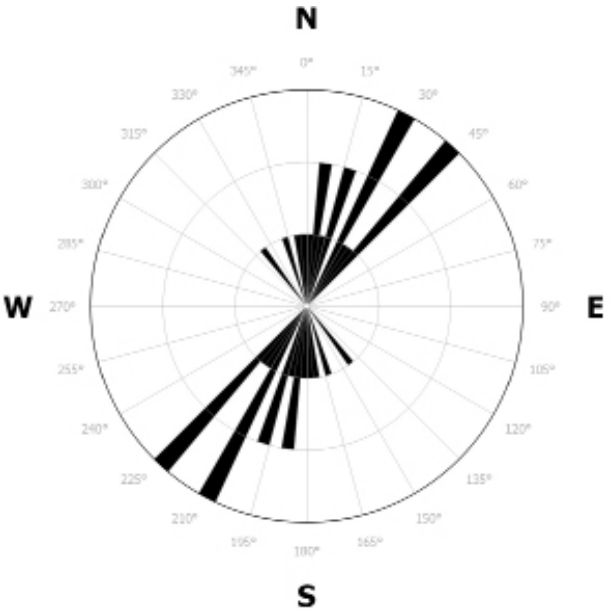

Fig. 5. Paleocurrent measurements from FA 1 outcrop indicating NE (axial) fluvial sediment dispersal.

Fig. 6. Well-developed annual growth rings in petrified wood fragments obtained from the study area.

possibly confined by faults (in places). It is noted that given the relatively cold climate setting, fluvial dynamics are considered to have changed due to seasonal variations in water discharge (Johnson, 1984; Miall, 1996; Michaelsen and Henderson, 2000a). Further, the thin fining-upwards cycles observed in FA 1 outcrops (Fig. 4) coupled with the well-developed overbank deposits (FA2) might suggest a non-perennial fluvial system, characterized by short discharge periods, as common in cold climate settings (Miall, 1996). Additionally, a flashy run off regime is also commonly observed within late Permian fluvial deposits in coal-bearing sub-basins in the South Gobi region. Furthermore, an interesting new significant study of 64 million kilometers of modern rivers around the world, reveals that between 51% and 60% stop flowing periodically or dry-up for part of the year (Messager et al., 2021). While this study empirically quantified and mapped the global distribution of modern non-perennial rivers and streams, similar data is clearly lacking for the Permian system. Nevertheless, non-perennial rivers are considered here to have played an important role during Permian times.

Facies 2: Overbank

Facies 2 is characterized by light to dark grey siltstone, carbonaceous mudstone and subordinate fine to medium grained light grey sandstone, often inter-bedded or inter-laminated. Sedimentary structures are dominated by horizontal and indistinct bedding with subordinate ripple lamination. This facies seldom outcrop in the study area, but is well represented in the drillcore record. Organic

debris from peat forming plants is common in this facies, including indeterminate fragmentary plant axes, and imprints of *Koretrophyllites* (Rigby, pers. com).

Facies 2 is interpreted as proximal-distal overbank and floodbasin deposits, based on its overall fine grain-size, sedimentary structures and plant fossils (Table 2). Similar deposits were documented in the late Permian Moranbah- and Rangal Coal Measures in the northern Bowen Basin, Australia by Michaelsen and Henderson (2000) and Michaelsen et al. (2000), respectively. It is noted that *Koretrophyllites* occurs prolifically in the large Permo-Carboniferous Tungusska Coalfield of Siberia (Mironov, 1964). It probably grew in tufts similar to extant reeds and rushes around bogs, marshes and swamps. *Koretrophyllites* occupied the same niche as *Phyllotheca* did in the Permian of Australia (Rigby, pers. com).

Facies 3: Peat mire

Facies 3 is composed of high ash black bituminous coaland commonly inter-finger with carbonaceous mudstone, siltstone and sandstone of FA 2. Facies 3 is very well developed within the study area; with apparent net thickness of individual seams up to 19.45 m. The thickest seam (often characterized by numerous splits) is preserved in the basal part of the coal measures. With regards to stacking patterns, FA 3 is commonly immediately underlain and overlain by FA 2 deposits. The drill core record typically shows very broken coal characterized by gravel size fragments, preventing detailed mm-scale brightness logging. However, vitrinite-rich fragments were commonly observed and recorded during the core logging process.

Facies 3 is considered to represent laterally extensive (c. 20 km strike length), low-lying peat mire systems developed on the lower coastal plain.). The sedimentary record indicates the coal-bearing package contains up to eight master coal-bearing intervals within the study area. The master coal-bearing intervals may consist of a single seam or a larger number of seam splits which are within vertical succession and which are laterally interconnected (Michaelsen and Henderson, 2000a). The borehole record in concurrence with the downhole geophysical logs shows the coal/clastic ratio is 0.0867, somewhat similar to the middle Permian Tavan Tolgoi deposit in southern Mongolia (Michaelsen and Storetvedt, 2024).

Fig. 7. Example of rapid coal seam thickness change and wedge shape geometry from a relatively deep trench within the eastern sector of the study area.

Table 4. Summary of proximate analytical results from 82 samples from drill cores (ie. mainly targeting the economically important basal seam) and 3t bulk sample from trial shaft. Coal quality data from Tavan Tolgoi, Nariin Sukhait and Gurvantes from Erdenetsogt et al. (2009).

	Total Moisture % (arb)	Residual Moisture % (adb)	Ash % (db)	Volatile Matter % (db)	Fixed Carbon % (db)	Gross CV kcal/kg (daf)	Net CV kcal/kg (adb)	Sulphur % (db)	CSN
Drill core database									
Range	0.99 - 32.79	0.32 - 8.55	26.07 - 58.58	5.54 - 18.21	17.57 - 65.06	5,636 - 8,716	1,369 - 6,417	0.1 - 1.92	0 - 4.50
Average	13.43	1.74	46.95	10.46	41.35	7,772	4,001	0.51	0.32
3 t bulk sample									
Average	7.9	0.73	43.45 (adb)	8.52 (arb)	47.3 (adb)	8,527	4,274 (arb)	0.48 (adb)	0.5 - 1.5
South Gobi Basin (Permian)									
Tsagaan Tolgoi 700 series		5.51	13.53	35.07 (daf)		7,278.43		0.88	
Tsagaan Tolgoi 500 series		4.9	20.77	31.64 (daf)		6,725.12		0.72	
Tsagaan Tolgoi 100 series		1.77	32.73	33.64 (daf)		7,504.95		0.6	
Tavan Tolgoi seam 13		2.1 (db)	27.00	34.20 (daf)		7,791.40		0.7	
Tavan Tolgoi seam 9		0.5 (db)	24.60	30.10 (daf)		8,054.30		0.7	
Tavan Tolgoi seam 8		0.6 (db)	24.00	29.80 (daf)		8,054.30		0.7	
Tavan Tolgoi seam 4		0.5 (db)	21.50	26.30 (daf)		8,054.30		0.7	
Tavan Tolgoi seam 3		0.6 (db)	19.90	25.90 (daf)		8,221.60		0.7	
Tavan Tolgoi seams 0 + 1		0.5 (db)	25.10	23.10 (daf)		8,006.50		0.7	
Nariin Sukhait seam 5		1.0 (db)	12.50	33.20 (daf)		7,743.60		0.5	
Gurvantes seam 1		2.3 (db)	20.70	34.30 (daf)		7,767.50		0.9	

The coal seams have a maximum development within the 2,223 hectares study area with the number of seams decreasing along strike to the northeast and southwest, with only two-three regionally continuous seams over the c. 20 km strike length. Coal quality data from relinquished exploration tenements to the northeast and southwest of the study area show consistent high ash content along strike.

Given the relatively cold depositional setting the thick basal seam (ie. up to 19.45 m net apparent thickness) is considered to represent a relatively long-lived peat mire system. McCabe (1987) estimated peat accretion rates to vary from 2.3 mm/pa in the tropics to 0.1 mm/pa in arctic regions. The wedge-shaped architecture of the coal seams evident from trenches and the drillhole record strongly argue for syn-tectonic deposition with irregular subsidence due to a sequence of active transtensive wrench faults / growth faults (Fig. 7).

In terms of coal quality of FA 3, a total of 82 coal samples from drill cores were analyzed at the SGS laboratory in Ulaanbaatar for proximate, CV, relative density and coking properties (Table 4). It is noted that a number of these samples were obtained from semi-oxidized coal due to the shallow nature of the exploration drilling and as such somewhat influenced the coal quality results. Total moisture content from the coal core samples is often relatively high (up to 32.79% arb with average of 13.43%), as the coal act as an aquifer in much of the study area. However, it is noted that the residual moisture is low with an average of 1.74 % (adb) which is similar to some Permian coal seams in South Gobi (eg. the 100 series at Tsagaan Tolgoi, seam 13 at Tavan Tolgoi and the Gurvantes seam), wehereas other South Gobi coals are characterized by lower values (Table 4).

A 3t bulk sample from a 35 m deep trial shaft, sunk proximal to drillhole DH14 (Fig. 2), was used for washability testing by Sedgeman. Interestingly the intersected coal in the shaft was relatively hard and coherent, unlike the gravely nature of the coal in the drill cores. The results from analysis of the 82 coal core

Table 5. Summary of ultimate analytical results from 3t bulk sample.

3t bulk sample	Carbon % (daf)	Hydrogen % (daf)	Nitrogen % (daf)	Sulphur % (daf)	Oxygen % (daf)
	91.1	4.4	2	0.6	1.9

Table 6. Summary of ash analysis results from 3t bulk sample

3t bulk sample	Al_2O_3	BaO	CaO	Cr_2O_3	Fe_2O_3	K_2O	MgO	MnO	Na_2O	P_2O_5	SiO_2	SrO	TiO_2
	14.1	0	0.7	0.01	1.35	4.4	0.3	0.01	0.22	0	77.00	0	0.7

samples are summarized in Table 4, and proximate and ultimate results from the 3t bulk sample are summarized in Tables 4 and 5 with ash composition disclosed in Table 6.

Raw head results from the 3t bulk sample shows the coal is rather high in ash (43.45% adb), with low inherent moisture (0.73% adb), low volatiles (8.52% adb), and relatively low sulphur (0.48% adb / 0.6% daf) with very high gross CV (8,527 kcal/kg daf). These results are consistent with the results from the 82 drill core samples as shown in Table 4. Moreover, the low inherent moisture and gross CV are in line with a number of Permian coals in the South Gobi region (Table 4 for comparison).

The content of volatile matter varies from 5.54-18.21% (db) in the 82 drill core samples with an average of just 10.46% (db), comparable with the results from the 3t bulk sample (Table 4). In comparison, Erdenetsogt et al., 2009 disclosed volatile matter values from three Permian coal-bearing sub-basins in the South Gobi (ie. seams 0, 1, 3, 4, 8, 9 and 13 from Tavan Tolgoi, seam 5 from Gurvantes and seam 1 from Nariin Sukhait - their Table 4). Their results show volatile matters in the nine Permian coal seams vary from 23.1 to 34.3% (daf) with an average of 29.6% which is c. three-fold the average values at Bayanjargalan (Table 4).

The very low volatiles results from some core samples (ie. as low as 5.54% db) are considered to reflect proximal sills (ie. devolatilization). Relatively thin dikes were intercepted by drilling and also documented by Erkhembaatar et al. (1995) in the four Permian stratigraphic units, but are not well exposed in the landscape. Given the scattered and shallow nature of the 38 exploration drill holes (Table 3) there is very limited data on the spatial distribution of the felsic intrusives. In this context, a large-scale investigation (ie. using data from >8,000 drill holes), examining changes in coal quality caused by sills and dolerite dykes in a coal mine in northeastern South Africa, Bussio and Roberts (2016) discovered an absence of a linear relationship between coal quality and proximity of intrusives. Bussio and Roberts (2016) noted that the relationship between intrusive sills, dykes and coal is complex and factors other than intrusion width must be considered in relation to the contact metamorphic effect.

The average ash content from the 82 drill core samples is 46.95% (db) is similar to the 43.45% (adb) from the bulk sample (Table 4). The consistent very high ash values are unusual for Permian coals in Mongolia. In comparison, Erdenetsogt et al., (2009) disclosed ash values from three Permian coal-bearing sub-basins in the South Gobi (ie. seams 0, 1, 3, 4, 8, 9 and 13 at Tavan Tolgoi, seam 5 at Gurvantes and seam 1 at Nariin Sukhait - their Table 4). The ash content of the seams varies from just 12.5 to 27 % (db) with a moderate average of 21.91% (db) (Table 4). It is noted that this average is very almost identical to the average from three late Permian coals at Tsagaan Tolgoi (ie. 22.34% db - Table 4).

The average coking properties from the 82 coal core samples is very low at 0.32 CSN, with the maximum recorded CSN of 4.5 in drillhole DH9R (Table 4).

The overall coal quality results indicate the coal would produce a high ash, low volatiles bituminous to semi-anthracite type of product, with low coking properties, low sulphur and nitrogen levels, and high gross CV. Similar high ash Permian coal deposits are very common in India (Tiwari et al., 2017; Kumar et al.,

Table 7. Ash yield simulation results from the Sedgeman study

Raw / Washed	Ash % (adb)	Yield % (arb)	Total Moisture % (arb)	Fixed Carbon % (arb)	Volatiles % (arb)	Gross CV kcal/kg (arb)	Net CV kcal/kg (arb)
Raw	43.5	100	7.9	44	7.9	4,430	4,274
Washed	31.9	54.4	9.4	52	9.4	5,230	5,056
Washed	30	49.3	9.6	53.3	9.6	5,365	5,188
Washed	25	35.5	10.1	56.8	10.2	5,716	5,532
Washed	20	23	11	60	10.8	6,037	5,845
Washed	18	18.6	11.5	61.1	11	6,150	5,953

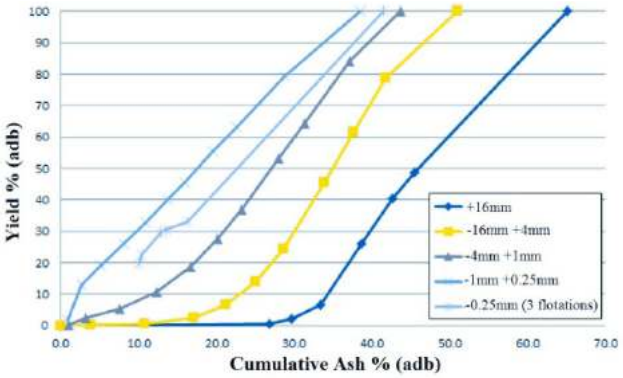

Fig. 8. Cumulative ash vs yield curves from the 3t bulk sample obtained from inclined shaft proximal to drillhole DH14 (Fig. 2).

2018; Kamble et al., 2019; Naik et al., 2021) with numerous power stations developed at mine mouths. Given the low yields from the Sedgeman washability test (Table 7, Fig. 8) a mine mouth boutique power station should thus be considered in order to develop the deposit. If the coal is used for power generation, the low volatile contents would mean lower quantities of flue gas would be generated, (ie. a relatively clean coal with less pollutants being released into the atmosphere). Further, the high hardgrove grindability index (>100) would also be lowering power station pulverizing requirements. The washability testing by Sedgeman showed that high ash deformation temperatures (>1,400^{0}C) would allow for high temperature boiler operation, delivering greater efficiency and lower capital cost on any future boutique mine mouth power plant construction. Source rock composition was determined by the ratio of oxides of Al and Ti from the 3t bulk sample (Table 6). According to Hayashi et al. (1997), if the Al_2O_3/TiO_2 ratio is <8, the source is considered to be mafic, if >20 it is felsic, and if it is between 8 and 21, the source rock is considered to have an intermediate composition. The results from the 3t bulk sample show an Al_2O_3/TiO_2 ratio of 19.79. Hence, using the scheme of Hayashi et al. (1997) it can be assumed that during peat accumulation, minerals and detrital sediments were accumulated from source rocks with an intermediate composition.

Succeeding the Sedgeman washability testing, Bureau Veritas (BV) Mongolia completed wet and dry pre-treatment analysis on two 24 kg samples from the basal seam obtained from the trial shaft (Table 8). The project was extended to include washability analysis at F1.60. The purpose of the project was to determine whether dry screening process would assist in the reduction of the consistently very high ash content of the coal from mid-40% to a range of somewhere in the mid-30%. The size by ash analysis showed only a slight improvement in the data for the lower size fractions when the sample was wet sized. The washability data indicated that the coal can be easily washed when required, however, at low yields (Table 8). Clean coal analysis shows that the basal coal seam cleans up extremely well (Table 9).

Table 8. Washability and liberation results from BV washability test

-11.2 mm+ 1.0 mm Fraction (air-dried)						
Mass % of Overall Sample		Fractional Results			Cumulative Results	
	Fraction	Mass	Yield	Ash	Mass	Ash
		(g)	%	%	%	%
47.4	F 1.60	2545	29.4	24.8	29.4	24.8
	S 1.60	6097	70.6	59.3	100	49.1
- 1.0 mm + 0 mm Fraction (air-dried)						
Mass % of Overall Sample		Fractional Results			Cumulative Results	
	Fraction	Mass	Yield	Ash	Mass	Ash
		(g)	%	%	%	%
52.6	F 1.60	3704	37.9	18.1	37.9	18.1
	S 1.60	6071	62.1	52.8	100	39.7
- 11.2 mm + 0 mm Fraction (air-dried)						
Mass % of Overall Sample		Fractional Results			Cumulative Results	
	Fraction	Mass	Yield	Ash	Mass	Ash
		(g)	%	%	%	%
100	F 1.60	6249	33.9	20.9	33.9	20.9
	S 1.60	12168	66.1	56.1	100	44.2

Table 9. Clean coal analysis results from the BV washability test

F1.60 Clean Coal Analysis (ad %)					
Sample ID	Moisture	Ash	Volatile Matter	Calorific Value kcal/kg	CSN
M2019	1	21.6	11.4	6,713	1.5
M2020	0.9	20.9	11.4	6,761	1.5

Facies 4: Gravely beachface

Facies 4 is composed of clast-supported, extra-formational, polymict conglomerate up to 3.1 m in thickness. The conglomerate beds extend outside the study area to the northeast and southwest over a strike length of c. 20 km. The clasts are well-rounded, and medium-large clasts (up to 10.3 cm in length) are predominantly elongate (Michaelsen, 2016, Fig. 5B). The pebble - cobble size clasts are primarily light to dark grey with common well developed plagioclase phenocrysts in a micro- crystalline matrix. Quartz clasts are relatively rare (<5%).

Facies 4 is interpreted here to represent gravely beachface deposits, developed along the shoreline of the elongate NE trending Permian seaway. Three laterally extensive gravely beach deposits are developed within the sub-basin, extending along strike for c. 20 km. Additional, but laterally restricted, FA 4 deposits are preserved north of the study area, possibly reflecting preservation of higher amplitude base-level changes in a setting with diverse depositional dynamics. The quartz content within exposed gravely beachface deposits in the study area is probably underrepresented in terms of larger quartz clasts, which might well have been removed for construction of abundant prehistoric burial mounds in the far southern part of the sub-basin, primarily made up of larger quartz clasts.

Waves and currents are considered to have transported the extra-formational clasts onshore as well as longshore during transgressive events (Clifton, 1973, 2003; Postma and Nemec, 1990; Reading and Collinson, 1996). The Canterbury Plains, New Zealand, provide a modern analog for ancient conglomeratic deposits in a high energy environment (Leckie, 1994, 2003). The Cretaceous Cardium Formation in Canada is considered to be an example from the rock record (Hart and Plint, 1989, 2003). However, it is highlighted here that every depositional system is unique with distinctive attributes.

Facies 5: Tidal flat

Facies 5 is characterized by inter-bedded to inter-laminated fine-grained sandstone and carbonaceous mudstone which are commonly bioturbated. The drill hole record shows Facies 5 reach a maximum thickness of 5 m (ie. from 192.8-197.8 m in DH02). Facies 5 is in places abruptly overlain by FA 4 deposits, separated by a sharp undulating bounding surface. Depositional structures include tidal bundels, wavy, disturbed, lenticular and parallel bedding, as well as scour and fill structures (Michaelsen, 2016, Fig. 5C). The bioturbation intensity index is moderate in places (ie. 3 in the scheme of Bann and Fielding, 2004). The biogenic structures are characterized by a low diversity assemblage of sand-filled *Planolites* and inclined ichno fossil structures up to 1.6 cm in length.

Facies 5 is interpreted as tidal flat deposits, developed along the late Permian shoreline of an elongate seaway. It bears a striking similarity to the modern North Sea tidal flat deposits documented by Reineck and Singh (1980), late Permian tidal flat deposits preserved in the Bowen Basin, Australia (Michaelsen and Henderson, 2000a) and early Permian marginal marine deposits in southern India recently documented by Saha et al. (2022). Furthermore, heterolithic tidal flat deposits were also documented and sampled in the Delgersogt area c. 200 km to the southwest as well as in the Binder district to the northeast, indicating widespread and prolonged tidal conditions along the seaway. The *Planolites* ichno fossils are unlined burrows infilled with sediments having textural and fabricational characters unlike those of the host rock (Pemberton and Frey, 1982). The relatively simple burrows were probably produced by benthic organisms, and the environmental habitat ranges from shallow to deep marine deposits to continental. Nonetheless, combined with other sedimentary structures such as wavy and lenticular bedding, this facies is considered to represent low energy inter-tidal deposits.

Facies 6: Shallow marine

Facies 6 is composed of horizontal bedded well-sorted fine to very fine-grained sandstone and minor siltstone. This facies has mainly been identified from sporadic outcrops, and the best preserved occur in the southern part of the study area at the base of the coal measures; a subdued and very fragmented sandstone strike ridge. The north-northeast oriented ridge extends over c. 780 m strike length and c. 25 m width, and is characterized by well sorted very fine-grained planar bedded sandstone. Individual sandstone beds are thin to medium (ie. up to 19 cm). Bedding dips along this strike ridge varies from 16-27° towards the southeast, with dips steepening towards the northern part of the strike ridge. Importantly, these deposits include a c. 8-19 cm thick very fragmented shellbed within a well-sorted very fine-grained sandstone matrix (Fig. 9). The shell bed has been extensively sampled from 2012-2023 for macrofossil analysis and petrological studies. Recent mapping work

Fig. 9. Example of FA 6 shellbed from the base of the late Permian coal measures showing an assemblage of taxodont bivalves and Archaeogastropods

Fig. 10. Fragmented exposures of well-developed wave ripples within FA 6 deposits proximal down dip of the basal coal seam (ie. exposed in trench) and along strike of the shellbed. The minor bedforms were probably generated by gentle swash and backwash currents in a low energy epicontinental seaway shoreface environment, with crestal spacing ranging from 0.7-1.1 cm. Compass for scale

proximal southwest of the study area shows that the shellbed sporadically outcrops over several kilometers along strike at the base of the coal measures, and might continue further along strike to the northeast. The shellbed is dominated by cold-resistant relatively robust archaeogastropod, taxodont bivalve taxa with rare fragmented *conulariida*. The vast majority of shells are articulated. The shellbed horizon includes occasional indeterminate petrified wood stems up to 9.6 cm in length.

Michaelsen (2016) reported that this facies also includes rare moderately developed crystal clusters of glendonites with individual glendonite structures up to 2.2 cm in length. In the northeastern part of the study area, along strike of the shellbed ridge, *Ophiomorpha* trace fossils (up to 9.8 cm in length) occur in a minor FA 6 outcrop characterized by well-sorted fine-grained sandstone. The vertical-inclined burrows are intermittently lined with ovoid pellets, typically 4-6 mm in diameter. Furthermore, these very fragmented outcrops of FA 6 include elongate, possibly chemoautotrophic, deep burrows of *solemyidae* bivalves. Dickins (1999) reported a similar type of bivalves from the middle Permian Khuff Formation in Oman.

The sandstone units generally consist of well sorted, fine-grained sandstone with angular to subangular framework grains with moderate to low sphericity. Sandstone petrology work shows textural immaturity, first cycle quartz dominance, with subordinate feldspar and lithics with common porphyry textures. Quartz grains commonly display recognizable crystal faces (ie. euhedral to subhedral morphology), as well as resorbed outlines and embayment's. FA 6 sandstone data plot within the recycled orogen provenance field of Dickinson (1985).

Lower flow regime generated symmetrical wave ripples, oriented NE-SW, were documented at a rare FA 6 outcrop proximal to a coal trench and drillhole DH4 (Fig. 10). Crestal spacing varies from 0.7-1.1 cm indicating a relatively low energy environment during deposition.

Facies 6 is interpreted as shallow marine deposits (Table 2). Water circulation within the relatively narrow and shallow Permian seaway might have resulted in low oxygen levels in some parts, hence the rare occurrences of macrofossils observed within the study area.

The symmetrical wave ripple structures were probably generated by swash and backwash currents proximal to the NNE oriented paleoshoreline with the two-way currents producing lower flow regime symmetrical ripple marks with pointed crests and rounded troughs. The prevailing wind direction was probably perpendicular to the wave ripples (ie. 100°-280°) the same direction as an uncovered petrified tree log in the northwestern part of the study area.

The taxodont bivalve and archaeogastropod dominated assemblage of the shellbed probably occupied a marginal shallow water habitat somewhat comparable to the Permian bivalve-dominated assemblage documented by Simões et al. (2016) from the Paraná Basin in Brazil.

The rare occurrence of glendonites initially reported by Michaelsen (2016) is consistent with

the boreal setting advocated by Manankov et al. (2006). As a variety of calcite, glendonites are considered to have a relatively low preservation potential, in this context the exposed glendonites within FA 6 also show clear signs of erosion. Selleck et al. (2007) noted that ancient glendonites may have value as recorders of the isotopic character of the waters from which the primary ikaite precipitated if primary carbonate signatures can be extracted.

The *Ophiomorpha* discovered in the northeastern part of the study area is a substrate-controlled ichnotaxon, found mainly in fine- to medium-grained sand deposits (Miller et al., 1998; Nagy et al., 2016). The trace fossils are the dwelling burrows of decapod crustaceans, and common in marine shoreface environments (Uchman, 1995; Parihar et al., 2016). In a sequence stratigraphic context, trace fossil associations have been used to characterize discontinuity surfaces (particularly at sequence boundaries) mainly based on the recognition of substrate-controlled ichnofacies (Nagy et al., 2016).

Depositional setting

There is every reason to believe that wrench tectonics played a critical role during late Permian times in Mongolia, where a sequence of related transtensive sub-basins formed along reactivated primordial fault systems. Some of these sub-basins became the locus for substantial tracts of peat accumulation (Michaelsen and Storetvedt, 2023; Storetvedt and Michaelsen, 2024). Overall, the c. 2,600 m thick sub-basinal infill within the wider study area records a protracted transition from shallow marine and humid coal forming depositional environments during the late Permian to relatively arid desolate terrestrial conditions during early Triassic times (Michaelsen and Storetvedt, 2024).

The rapid thickness variations and unstable nature of the coal seams documented within the study area suggest a syn-tectonic influence on peat deposition, considered here to be primarily driven by active wrench faults with a vertical component.

Rapid thickness changes are illustrated in a relatively deep trench (Fig. 7), where the coal seam rapidly thickens over a few meters and is characterized by wedge-shape geometry, which is common among Permian coal measures in Mongolia. Another example of rapid coal thickness changes is provided by the shallow drill holes DH09 and DH09R (drilled only 10 m apart along strike - Table 3), which intersected 12.0 m and 19.75 m of (net) coal of the basal seam, respectively; a significant thickness increase of 64.58% over just 10 m. Fig. 11 shows a large number of seam splits of the thick basal seam horizon preserved in drillhole DH09, inter-bedded with clastic deposits (ie. proximal-distal overbank deposits and floodbasin fines of FA2), characterized by sharp, planar, non-erosional bounding surfaces).

The consistent high ash content within the coal seams (ie. average of 46.95% (db) from 82 coal core samples and 43.45% (adb) from the 3t bulk sample) is unusual for Mongolian

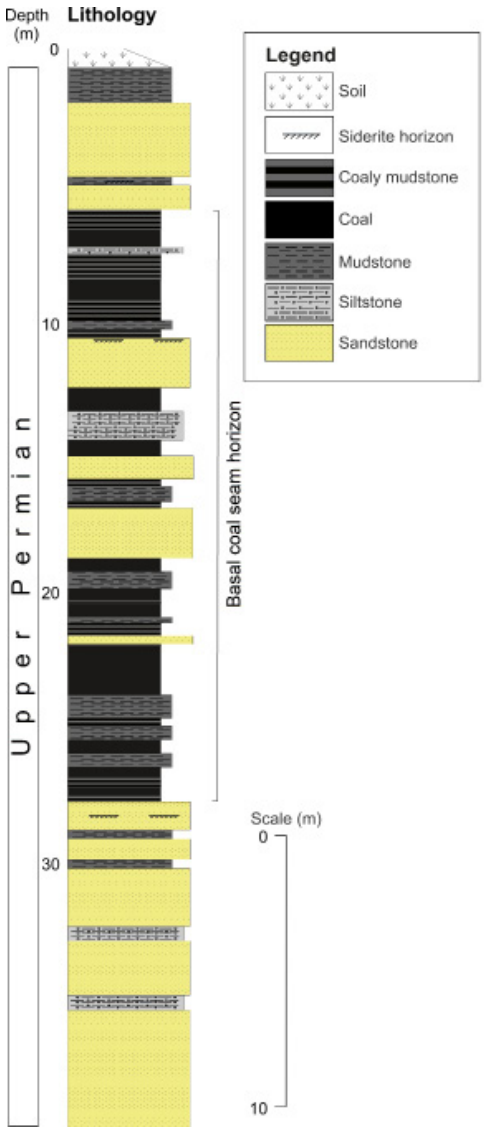

Fig. 11. Lithology log of drillhole DH09 showing numerous splits of basal high ash coal seam horizon

coals of Permian age. Erdenetsogt et al. (2009) disclosed average ash content of just 21.91% (db) from nine Permian coal seams from three sub-basins situated in the South Gobi Basin (Table 4). The high ash content is considered to have been primarily caused by the syn-tectonic depositional environment where active growth faults generated depressions in the landscape which were in turn infilled by an admixture of organics and clastic sediments as indicated by the numerous seam splits represented in Fig. 11. The high ash content might partly be caused by an influx of very fine grained windblown clastics, linked to the proximity of the seaway where the smooth water surface (and limited friction) might have accelerated the flow of wind (Fig. 12).

Overall, the climate warmed throughout the Perminan towards the End-Permian Extinction (EPE) (Ross and Ross, 1994). However, detailed recent work on Lopingian strata in the Bowen Basin, NE Australia, by Fielding et al. (2022), indicate that "the studied succession does not record a simple monotonic change in palaeoenvironmental conditions, but rather a series of intermittent stepwise changes towards warmer, and more environmentally stressed conditions leading up to the EPE". More recent work by Fielding et al. (2023) shows P3 and P4 glaciations are younger than previously thought, with P4 glaciation lasted until 254.5 Ma, with Fielding et al. (2022) noting that cold climate persisted until 253 Ma. The late Permian peat mire ecosystem documented by this study is considered to have developed during relatively cold-temperate climatic conditions along the southern shoreline of the Mongol-Transbaikalian Seaway. The epicontinental seaway had its opening to the northeast, towards the polar region of the time (Biakov et al., 2013; Michaelsen and Storetvedt, 2023), and thus may reinforce the possibility of a cool-temperate late Permian climate in northeastern Mongolia. The seaway and associated drainage

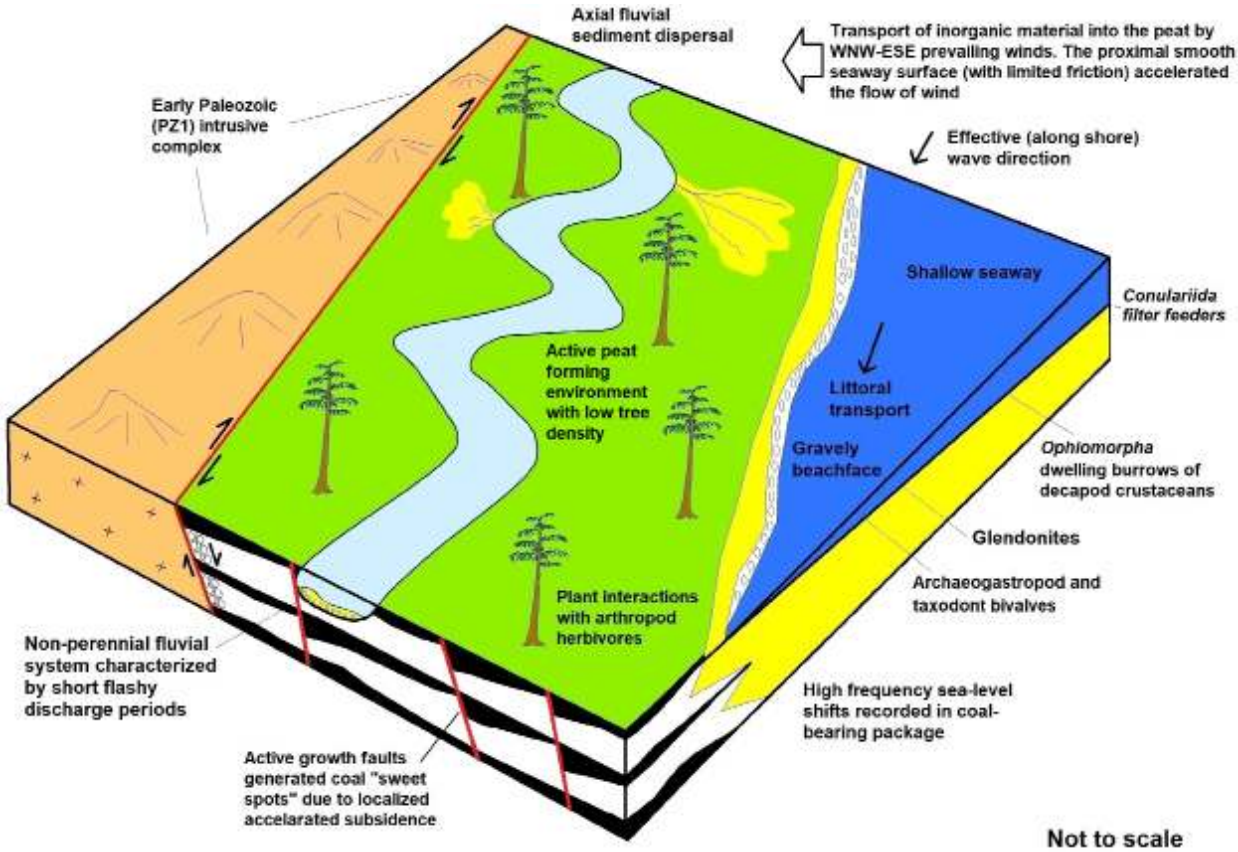

Fig. 12. Schematic depositional model for the emplacement of the very high ash late Permian coal measures (modified from Michaelsen and Storetvedt, 2023). Wedge-shaped coal "sweet spots" developed proximal to active growth faults generated by localized accelerated subsidence, however, these spots include numerous seam splits (Fig. 12) developed as a result of an influx of predominantly fine-grained clastics. Preliminary petrographic studies indicate the peat precursor of the basal seam was dominated by herbaceous plants and characterized by low tree density. Not to scale

systems were likely frozen during the dark, cold winter months.

The strongly developed annual growth rings in the petrified wood fragments (Fig. 6), coupled with the rare glendonite crystal clusters in FA 6 support the cold climate setting proposed by Manankov et al. (2006). However, it is noted here that glendonites (Selleck et al., 2007) are not univocally an indicator of low temperatures. An example is the c. 60 m thick Eocene Fur Formation in NW Denmark, deposited during super-greenhouse conditions close to the Paleocene-Eocene thermal maximum and containing very large glendonites up to 1.65 m across (Shultz, 2009; Schultz et al., 2020). In comparison the glendonites within the study area are tiny, reaching a maximum length of 2.2 cm. Nonetheless, the relatively cold depositional setting presented by this study is in line with detailed growth ring analysis on fossilized wood obtained from late Permian coal measures in the Tsagaan Tolgoi sub-basin in South Gobi by Cai et al. (2022), which suggested relatively short growing seasons. Furthermore, Cai et al. (2022) discovered a growth interruption, probably recording an early spring cooling event in a temperate climate. The results from this study coupled with the recent results from Cai et al. (2022) indicate relatively cold climatic conditions prevailed in both central and southern Mongolia during end late Permian times.

De Vleeschouwer et al. (2015) noted that few climate proxies provide information on paleo-wind directions. However, fossilized bedform elements such as wave-formed ripple marks can provide insight into the direction of flow that formed them. Wind directions might also be deduced from the preferred alignment of fallen tree trunks (Hayward and Hayward, 1995). However, only one petrified tree trunk with a diameter of 15 cm was uncovered during field work within the basal part of stratigraphic unit $P_2 cn_2$ in the northeastern sector of the study area. The modest tree trunk was embedded in organic-rich sandstone deposits and oriented 100°-280°, indicating WNW-ESE prevailing winds during the late Permian. It is noted that this direction is perpendicular to the symmetrical wave ripples documented in FA 6 sandstones.

The thick basal coal seam horizon probably represents a relatively significant time span, considering the slow growth in the cold-temperate climatic realm (McCabe, 1987; Diessel, 1992).

Extensive field work conducted along scattered outcrops of the Mongol-Transbaikalian Seaway from Adaatsag to Binder and strongly indicate the epicontinental seaway experienced several marked regressive events during the Permian, with the 420 m thick coal-bearing package from this study possibly representing one of the most significant regressive events. Alternatively, the seaway was backfilled to the Bayanjargalan district during deposition of the late Permian coal measures.

Late Permian sea-level fluctuations (ie. c. 0.75-3 Ma cycles) were coupled with restricted mountain glaciations according to Erwin, 1993, 1994; Ross and Ross, 1994. Sea-level fluctuations are also evident in the three logged sections of the Permian seaway by Manankov et al., 2006, (their Fig. 2). As an example, the Adaatsag section appears to contain a total of eight well-developed cyclothems with an average thickness of c. 100 m, and apparently spans over c. 7 Ma from the Sakmarian to Artinskian. Hence, each cyclothem could represent a time span of c. 1 Ma and as such might represent tectonic pulses. Adopting the apparent reasonable sedimentation rates from the Adaatsag section as a proxy, the c. 420 m thick coal measures of this study might represent a time span of c. 4 Ma, with the entire sub-basinal fill representing a prolonged period of c. 26 Ma. Given the c. 180 m thick transitional unit overlying the coal measures, the depositional window for the coal-bearing strata might be around 258-254 Ma. However, it is noted that every sedimentary basin is unique and sedimentation rates could well vary significantly from the Adaatsag district.

A new study by Michaelsen and Demberelsuren (in prep) indicate relatively low Tissue Preservation Index and moderate Gelification Index for the thick lower seam. The new results suggest the peat precursor of the basal seam evolved in a limnic (flood basin) setting dominated by herbaceous plants and characterized by low tree density. The flood-prone setting is in agreement with the

Table 10. Preliminary results from a new study by Michaelsen and Demberelsuren (in prep) showing striking similarities between the late Permian coal measures at Bayanjargalan and the coal-bearing Yamaan Us Formation (P_3yb) in the Tsagaan Tolgoi sub-basin in Southern Mongolia (see Fig. 1).

	Bayanjargalan	**Tsagaan Tolgoi**
Sub-basinal architecture	Elongate transtensive fault-bounded sub-basin warped into an assymetrical syncline during transpresssion	Elongate transtensive fault-bounded sub-basin warped into an assymetrical syncline during transpresssion
Structural complexity	Moderate	Relatively high
Thickness of Permo-Triassic fill	2,600 m	1,500 m
Age of Permian coal measures	Lopingian	Lopingian
Depositional setting	Syn-tectonic deposition on lower coastal plain	Lower coastal plain. Common base-level changes
Paleoclimate	Cold - temperate	Temperate with early spring cooling events
Thickness of coal measures	420 m	570 m
No. of master coal-bearing intervals	8	8
Location of thickest coal seam	Basal part of coal measures	Basal part of coal measures
Resource base	64-111 Mt Exploration Target	45 Mt and 150-250 Mt Exploration Target
Coal quality (in general)	Very high ash, low volatiles thermal coals	Low-moderate ash thermal coals
Ash composition of basal seam	77% SiO_2	71% SiO_2
Dominant macroflora	*Cordaites* gymnosperms	*Cordaites* gymnosperms
Petrified wood characteristics	Strongly developed annual growth rings	Strongly developed annual growth rings
Shallow marine fossils at base	Laterally continous shell bed. Rare *conulariida* fragment	Rare trilobite
Overlying transitional zone thickness	180 m	50-80 m
Coal Bed Methane potential	Gas-bearing coal potential along margins of depocenters	Gas-bearing coal confirmed by drilling

indicated flashy run off regime observed in fluvial outcrops within the study area (Fig. 4), considered here to mirror a non-perennial fluvial system, characterized by short discharge periods as common in cold climatic settings (Johnson, 1984; Miall, 1996; Michaelsen and Henderson, 2000a).

Generated by extensive field work on the late Permian coal-bearing Yamaan-Us Formation in the Tsagaan Tolgoi sub-basin, located c. 570 km south-southwest of Ulaanbaatar (Fig. 1), a new study by Michaelsen and Demberelsuren (in prep) shows a number of striking similarities with the current study area (see Table 10 for comparison). The similarities of the two widely separated sub-basins includes, but are not limited to; the same number of master coal-bearing intervals with the thickest at the base, comparable elevated $Si0_2$ ash content of the main thick basal seam, strongly developed annual growth rings in petrified wood, common siderite horizons, a lower coastal plain setting characterized by common base-level changes and both coal measures are conformably overlain by a 50-180 m thick transitional Permo-Triassic boundary zone (Table 10). As such, it is not unlikely that the two coal-bearing depositional systems developed synchronously and may have experienced similar tectonic, eustatic and climatic influences.

Further afield in NE Australia, Fielding et al. (2022) noted that the late Permian fossil floras indicate remarkably consistent terrestrial ecosystems throughout the late Lopingian until the EPE (see also Michaelsen et al., 1999; Michaelsen et al., 2000; Michaelsen, 2002). However, recent work by Michaelsen and Storetvedt (2024) from Mongolia indicate that fossil wood growth rings at Tsagaan Tolgoi shows a decrease in size towards the EPE, possibly indicating deteriorating growing conditions. The final collapse of the long-lived peat mire ecosystem at Tsagaan Tolgoi was protracted, with a 50-80 m thick transitional zone extending for an estimated c. 330-530 ky based on interpreted Milankovitch cyclicity. The coal measures at Bayanjargalan are conformably overlain by an uppermost late Permian c. 180 m thick transitional unit which is organic rich but coal-barren. This unit might represent a prolonged interval of c. 1.8 Ma if adopting the apparent sedimentation rates from the Adaatsag section of Manankov et al. (2006). The transitional unit contains a 60 cm thick calcareous mudstone bed possibly indicating warming conditions (Fan et al., 2021) towards the EPE.

Plant-arthropod interactions

Insects first appeared during the Carboniferous and experienced a dramatic increase in diversification during the Early Permian

(Labandeira, 2018). A comprehensive survey of Permian floras by McLoughlin et al. (2021) revealed over 400 discrete arthropod-herbivory-damage/plant-taxon/stratigraphic-unit associations from numerous sedimentary basins spanning all regions of Gondwana from the earliest Asselian to the latest Changhsingian. Recently, a systematic study of plant-insect interactions of Cathaysian flora by Feng et al. (2021) documented eight types of insect damage of five functional feeding groups present on 11 plant species in the early Permian Wuda Tuff Flora, located c. 20 km southwest of Wuhai in Inner Mongolia, China. However, plant-insect interactions have until now not been documented in detail from Permian flora in Mongolia.

Permian macroflora are preserved in several sub-basins in southern and central Mongolia (Durante, 1976; Orolmaa et al., 1999; Demberelsuren et al., 2023; Michaelsen and Storetvedt, 2024), and are identical to the central part of the Angara floral realm.

Carbonized leaf compressions are very rare within the study area. A concentration of well-preserved *Cordaites* leaf imprints were discovered and sampled during recent mapping work at a trench along the basal coal seam in the far southern part of the sub-basin (ie. proximal southwest of the current study area). Here oviposition lesions (DT228 in particular) from arthropod-plant interactions were observed on carbonized *Cordaites* leaf impressions (Labandeira, pers. com).

In the stratigraphic unit underlying the coal measures (Fig. 3), a series of six closely spaced oviposition lesions (DT246 in particular) were observed on a fossilized branch of a seed plant. The circular lesions are up to 10 mm in length (Fig. 13). It is noted that the oviposition lesions are almost twice the size of previous reported DT246 from riparian Taeniopteris foliage at the Colwell Creek Pond locality in north-central Texas, of uppermost Early Permian age (Schachat et al., 2014).

Fig. 13. Large oviposition lesions in late Permian petrified wood documented in the northern part of the study area (see text for discussion).

It is highlighted here that both petrified wood and carbonized leaf compressions occur very rarely within the study area, as such the evidence of plant-arthropod interactions on these rare occurrences might suggest relatively widespread plant-insect interactions within the study area and possibly along the paleoshoreline of the Mongol-Transbaikalian Seaway during late Permian times. Further research is clearly required in this field.

SUMMARY

- This study provided an overview of the petro-chemical characteristics and depositional setting of the late Permian high ash coal deposit preserved in the Bayanjargalan area in central Mongolia, drawing on a new integrated database.
- Paleoclimatic indicators indicate suggest that relatively cold conditions persisted during deposition of the coal-bearing strata.
- The persistent high ash values are uncharacteristic of Permian coals in Mongolia.
- The high ash values coupled with the rapid thickness variations and unstable nature of the coal seams strongly suggest a syn-tectonic influence on their development.
- Given the high ash values and the low yield results from washability testing, argue for construction of a boutique mine mouth power station in order to develop the coal deposit. The low volatile contents would mean lower quantities of flue gas would be generated in a power station (ie. a relatively clean coal product with less pollutants being released into the atmosphere).
- A number of striking similarities between the late Permian coal measures at Bayanjargalan and Tsagaan Tolgoi in South Gobi were noted. It is not unlikely that the two coal-

bearing depositional systems may have experienced similar tectonic, eustatic and climatic influences.

ACKNOWLEDGEMENTS

This paper is dedicated to the late Dr. John Rigby, QUT, to honor his immense contribution to paleobotany. Bureau Veritas Mongolia, and in particular Maria Grady, is greatly acknowledged for their assistance with the wet and dry pre-treatment and washability analysis. Two anonymous reviewers are greatly acknowledged for improving this contribution. The following experts are thanked for their assistance with identifying the Permian flora, fauna, trace fossils and plant-insect interactions: Dr. Yarinpil Ariunchimeg, Chair of Mongolian Commission on Stratigraphy, Dr. Conrad Labandeira, Department of Paleobiology, Smithsonian Institution, Professor Robert Henderson, James Cook University, Dr. Spencer Lucas, New Mexico Museum of Natural History and Science, Dr. William DiMichele and Dr. Thomas Waller, Smithsonian Institution, Professor Stephen McLoughlin, Swedish Museum of Natural History and Paleontology, Dr. Jenò Nagy, Department of Geosciences, University of Oslo, Associate Professor Mihai Popa, University of Bucharest, Dr. Mike Pole, Nanjing Institute of Geology and Paleontology, Dr. Sebastian Voigt, Urweltmuseum GEOSKOP, and Serge Naugolnykh, Institute of Geology, Russian Academy of Sciences.

REFERENCES

Bann, K.L., Fielding, C.R. 2004. An integrated ichnological and sedimentological comparison of non-deltaic shoreface and subaqueous delta deposits in Permian reservoir units of Australia. Geological Society, London, Special Publications, vol. 228(1), p. 273-310. https://doi.org/10.1144/GSL.SP.2004.228.01.13

Biakov, A.S, Goryacheva, N.A., Davydovb, V.I., Vedernikova, I.L. 2013. The First Finds of Glendonite in Permian Deposits of the North Okhotsk Region, Northeastern Asia. Geology, Doklady Akademii Nauk, vol. 451(3), p. 299-302. https://doi.org/10.1134/S1028334X13070210

Brand, U., Posenato, R., Came, R.E., Affek, H., Angiolini, L., Azmy, K., Farabegoli, E. 2012. The end-Permian mass extinction: a rapid volcanic CO_2 and CH_4-climatic catastrophe. Chemical Geology, vol. 322-323, p. 121-144. https://doi.org/10.1016/j.chemgeo.2012.06.015

Bridge, J.S. 1993. Description and interpretation of fluvial deposits: a critical perspective. Sedimentology, vol. 40(4), p. 801-810. https://doi.org/10.1111/j.1365-3091.1993.tb01361.x

Burgess, S.D., Bowring, S., Shen, S.Z. 2014. High-precision timeline for Earth's most severe extinction. PNAS, Earth, Atmospheric, and Planetary Sciences, vol. 111(9), p. 3316-3321. https://doi.org/10.1073/pnas.1317692111

Bussio, J.P., Roberts, J.R. 2016. A large-scale investigation into changes in coal quality caused by dolerite dykes in Secunda, South Africa-implications for the use of proximate analysis on a working mine. Journal of African Earth Sciences, vol. 117, p. 401-409. https://doi.org/10.1016/j.jafrearsci.2016.01.019

Cai, Y.F., Zhang, H., Feng, Z., Gou, X.D., Byambajav, U. Zhang, Y.C., Yuan, D.X., Qie, W.K., Xu, H.P., Cao, C.Q., Yarinphil, A., Shen, S.Z. 2022. A newconifer stem, Ductoagathoxylon tsaaganensis, from the Upper Permian of the South Gobi Basin, Mongolia and its palaeoclimatic and palaeoecological implications. Review of Palaeobotany and Palynology, vol. 304, 104719. https://doi.org/10.1016/j.revpalbo.2022.104719

Clifton, H.E. 1973. Pebble segregation and bed lenticularity in wave-worked versus alluvial gravel. Sedimentology, vol. 20(2), p. 173-187. https://doi.org/10.1111/j.1365-3091.1973.tb02043.x

Clifton H.E. 2003. Supply, segregation, succession, and significance of shallow marine conglomeratic deposits. Bulletin of Canadian Petroleum Geology, vol. 51(4), p. 370-388. https://doi.org/10.2113/51.4.370

Demberelsuren, B., Jargal, L., Munkhtsengel, B., Lkhagva-Ochir, S., Ganzorig, R., Tsolmon, A., Enkhbat, C., Turbat, E., Tuvshinbayar, E., Tugsjargal, A. 2023. Coal facies of the Middle Permian Baruunnaran deposit, South

Mongolia. Mongolian Geoscientist, vol. 28(57), p. 71-91. https://doi.org/10.5564/mgs.v28i57.3236

Demberelsuren, B., Jargal, L., Munkhtsengel, B. 2021. The coal facies interpretations in the Baruunnaran coal deposit, Southern Mongolia. School of Geology and Mining Engineering, MUST, Geology, vol. 36, p. 120-137.

De Vleeschouwer, D., Leather, D., Claeys, P. 2015. Ripple marks indicate Mid-Devonian paleo-wind directions in the Orcadian Basin (Orkney Isles, Scotland). Palaeogeography, Palaeoclimatology, Palaeoecology, vol. 426, p. 68-74. https://doi.org/10.1016/j.palaeo.2015.03.001

Dickins, J.M. 1999. Mid-Permian (Kubergandian - Murgabian) bivalves from the Khuff Formation, Oman: implications for world events and correlation. Rivista Italiana di Paleontologiae Stratigrafia, vol. 105(1), p. 23-36. https://doi.org/10.13130/2039-4942/5364

Dickinson, W.R. 1985. Interpreting Provenance Relations from Detrital Modes of Sandstones. In: Zuffa, G.C. (Ed.) Provenance of Arenites, NATO ASI Series, vol. 148, p. 333-361. https://doi.org/10.1007/978-94-017-2809-6_15

Diessel, C.F.K. 1992. Coal-bearing Depositional Systems. Springer-Verlag, Berlin, 721 p. https://doi.org/10.1007/978-3-642-75668-9

Durante, M.V. 1976. The Paleobotanical Basis for Stratigraphy of the Carboniferous and Permian of Mongolia. Proceedings of the Joint Soviet-Mongolian Geological Expedition, vol. 19, Moscow, Nauka.

Erdenetsogt, B.O., Lee, I., Bat-Erdene, D., Jargal, L. 2009. Mongolian coal-bearing basins: Geological settings, coal characteristics, distribution, and resources. International Journal of Coal Geology, vol. 80(2), p. 87-104. https://doi.org/10.1016/j.coal.2009.08.002

Erkhembaatar, H., Dorjsuren, B., Myagmarsuren, A. 1995. Geological Mapping Report 4825f.

Erwin, D.H. 1993. The Great Paleozoic Crisis. Columbia University Press, New York.

Erwin, D.H. 1994. The Permo-Triassic extinction. Nature, vol. 367, p. 231-236. https://doi.org/10.1038/367231a0

Fan, D., Shan, X., Makeen, Y.M. He, W., Su, S., Wang, Y., Yi, J., Hao, G., Zhao, Y. 2021. Response of a continental fault basin to the global OAE1a during the Aptian: Hongmiaozi Basin, Northeast China. Scientific Reports, vol. 11, 7229. https://doi.org/10.1038/s41598-021-86733-x

Feng, Z., Wang, J., Zhou, W.M., Wan, M.L., Pšenička, J. 2021. Plant-insect interactions in the early Permian Wuda Tuff Flora, North China. Review of Palaeobotany and Palynology, vol. 294, 104269. https://doi.org/10.1016/j.revpalbo.2020.104269

Ferm, J.C., Staub, J.R. 1984. Depositional controls of mineable coal bodies. In: Rahmani, R.A., Flores, R.M. (eds.) Sedimentology of Coal and Coal-Bearing Sequences. International Association of Sedimentologists, Special Publication, vol. 7, p. 275-289. https://doi.org/10.1002/9781444303797.ch15

Fielding, C.R., Frank, T.D., Birgenheier, L.P. 2023. A revised, late Palaeozoic glacial time-space framework for eastern Australia, and comparisons with other regions and events. Earth-Science Reviews, vol. 236, 104263. https://doi.org/10.1016/j.earscirev.2022.104263

Fielding, C. R., Frank, T.D., Savatic, K., Mays, C., McLoughlin, S., Vajda, V., Nicoll, R.S. 2022. Environmental change in the late Permian of Queensland, NE Australia: The warmup to the end-Permian Extinction. Palaeogeography, Palaeoclimatology, Palaeoecology, vol. 594, 110936. https://doi.org/10.1016/j.palaeo.2022.110936

Hansen, H.J., Lojen, S., Toft, P., Dolenec, T., Jinan, T., Michaelsen, P., Sarkar, A. 2000. Magnetic susceptibility and organic carbon isotopes of sediments across some marine and terrestrial Permo-Triassic boundaries. Developments in Palaeontology and Stratigraphy, vol. 18, p. 271-289. https://doi.org/10.1016/S0920-5446(00)80016-3

Hart, B.S., Plint, A.G. 1989. Gravelly shoreface deposits: a comparison of modern and ancient facies sequences. Sedimentology, vol. 36(4), p. 551-557. https://doi.org/10.1111/j.1365-3091.1989.tb02085.x

Hart, B.S., Plint, A.G. 2003. Stratigraphy and sedimentology of shoreface and fluvial conglomerates: insights from the Cardium Formation in NW Alberta and adjacent

British Columbia. Bulletin of Canadian Petroleum Geology, vol. 51(4), p. 437-464. https://doi.org/10.2113/51.4.437

Hayashi, K.L., Fujisawa, H., Holland, H.D. Ohmoto, H. 1997. Geochemistry of ~1.9 Ga sedimentary rocks from northeastern Labrador, Canada. Geochemica et Cosmochimica Acta, vol. 61(19), p. 4115-4137. https://doi.org/10.1016/S0016-7037(97)00214-7

Hayward, J.J. Hayward, B.W. 1995. Fossil forests preserved in volcanic ash and lava at Ihumatao and Takapuna, Auckland. Tane, vol. 35, p. 127-142.

Huang, C. Tong, J., Hinnov, L., Chen, Z.Q. 2011. Did the great dying of life take 700 k.y.? Evidence from global astronomical correlation of the Permian-Triassic boundary interval. Geology, vol. 39(8), p. 779-782. https://doi.org/10.1130/G32126.1

Jargal, L., Kuznetsova, A. A., Tserensodnom, P., Erdembat, L. 1990, Petrographic character of coals from major coal seam of Tavan Tolgoi deposit. In: Geology and Mineral deposits of Mongolian People's Republic, Nedra, Moscow, p. 158-163 (in Russian).

Johnson, D.P. 1984. Development of Permian fluvial coal measures, Goonyella, Australia. In: Rahmani R.A., Flores, R.M. (eds.) Sedimentology of Coal and Coal-Bearing Sequences, Special Publication, vol. 7, p. 149-162. https://doi.org/10.1002/9781444303797.ch8

Johnson, C.L., Amory, J.A., Zinniker, D., Lamb, M.A., Graham, S.A., Affolter, M., Badarch, G. 2007. Sedimentary response to arc-continent collision, Permian, southern Mongolia. In: Draut, A., Clift, P., Scholl, D. (eds.) Formation and Applications of the Sedimentary Record in Arc Collision Zones. GSA Special Papers, vol. 436, p. 1-26. https://doi.org/10.1130/2008.2436(16)

Kamble, A.D., Saxena, V.K., Chavan, P.D., Singh, B.D., Mendhe, V.A. 2019. Petrographic and chemical reactivity assessment of Indian high ash coal with different biomass in fluidized bed co-gasificatio. Journal of the Energy Institute, vol. 92(4), p. 982-1004. https://doi.org/10.1016/j.joei.2018.07.007

Kumar, A. Singh, A.K., Singh, P.K., Singh, A.L., Jha, M.K. 2018. Demineralization Study of High-Ash Permian Coal with Pseudomonas mendocina strain B6-1: A Case Study of the South Karanpura Coalfield, Jharkhand, India. Energy Fuels, vol. 32(2), p. 1080-1086. https://doi.org/10.1021/acs.energyfuels.7b02562

Labandeira, C.C. 2018. The Fossil History of Insect Diversity. In: Foottit, R.G., Adler, P.H. (eds.) The Fossil History of Insect Diversity, p. 723-788. https://doi.org/10.1002/9781118945582.ch24

Leckie, D.A. 1994. Canterbury Plains, New Zealand - implications for sequence stratigraphic models. American Association of Petroleum Geologists Bulletin, 78(8), p. 1240-1256. https://doi.org/10.1306/A25FEABD-171B-11D7-8645000102C1865D

Leckie D.A. 2003. Modern environments of the Canterbury Plains and adjacent offshore areas, New Zealand - an analog for ancient conglomeratic depositional systems in nonmarine and coastal zone settings. Bulletin of Canadian Petroleum Geology vol. 51(4), p. 389-425. https://doi.org/10.2113/51.4.389

Li, J., Zhang. J. 2017. Sequence Stratigraphy of Fluvial Facies: A New Type Representative from Wenliu Area, Bohai Bay Basin, China. Seismic and Sequence Stratigraphy and Integrated Stratigraphy - New Insights and Contributions. https://doi.org/10.5772/intechopen.71149

McCabe, P.J. 1987. Facies studies of coal and coal-bearing strata. Geological Society, London, Special Publications, vol 32, p. 51-66. https://doi.org/10.1144/GSL.SP.1987.032.01.05

McLoughlin, S., Prevec, R., Slater, B. 2021. Arthropod interactions with the Permian Glossopteris flora. Journal of Palaeosciences, vol. 70(1-2), p. 43-133. https://doi.org/10.54991/jop.2021.11

Manankov, I.N. 1998. Late Permian productida (Brachiopoda) from southeastern Mongolia. Paleontological Journal, vol. 32, p. 486-492.

Manankov, I.N. 1999. Reference section and upper Permian zonation in Southeastern Mongolia. Stratigrafia i Geologicheskaya Korrelyatsia, vol. 7(1), p. 56-65.

Manankov, I.N., Shi, G.R., Shen, S.Z. 2006. An overview of Permian marine stratigraphy and

biostratigraphy of Mongolia. Journal of Asian Earth Sciences, vol. 26(3-4), p. 294-303. https://doi.org/10.1016/j.jseaes.2005.11.008

Manankov, I.N. 2012. Brachiopods, biostratigraphy, and correlation of the Permian marine deposits of Mongolia. Paleontological Journal, vol. 46(12), p. 1325-1349. https://doi.org/10.1134/S0031030112120040

Messager, M.L., Lehner, B., Cockburn, C., Lamouroux, N., Pella, H., Snelder, T., Tockner, K., Trautmann, T., Watt, C., Datry, Th. 2021. Global prevalence of non-perennial rivers and streams. Nature, vol. 594, 391-397. https://doi.org/10.1038/s41586-021-03565-5

Miall, A.D. 1996. The Geology of Fluvial Deposits. Sedimentary Facies, Basin Analysis and Petroleum Geology. Springer Verlag, Berlin, 582 p.

Michaelsen, P. and Demberelsuren, B. (in prep). Maceral analysis, petro-chemical composition and cross-basin correlation of two late Permian coal deposits in central and southern Mongolia. Mongolian Geoscientist.

Michaelsen, P., Storetvedt, K.M. 2024. Protracted destabilization and collapse of peat mire ecosystems at the Permo-Triassic boundary recorded by a sequence of related transtensive sub-basins in central and southern Mongolia. Permophiles, vol. 76, p. 46-51. https://permian.stratigraphy.org/files/permophiles/Permophiles%2076.pdf.

Michaelsen, P., Storetvedt, K.M. 2023. Tectonic evolution of a sequence of related late Permian transtensive coal-bearing sub-basins, Mongolia: A global wrench tectonics portrait. Mongolian Geoscientist, vol. 28(57), p. 1-53. https://doi.org/10.5564/mgs.v28i57.3200

Michaelsen, P. 2016. Late Permian coal formation under boreal conditions along the shores of the Mongol-Transbaikalian seaway. New Concepts in Global Tectonics Journal, vol. 4(4), p. 615-636.

Michaelsen, P. 2002. Mass extinction of peat-forming plants and the effect on fluvial styles across the Permo-Triassic boundary, Bowen Basin, Australia. Palaeogeography, Palaeoclimatology, Palaeoecology, vol. 179(3-4), p. 173-188. https://doi.org/10.1016/S0031-0182(01)00413-8

Michaelsen, P., Henderson, R.A., Crosdale, P.J., Fanning, C.M. 2001. Age and significance of the Platypus-Tuff Bed, a regional reference horizon in the Upper Permian Moranbah Coal Measures, north Bowen Basin. Australian Journal of Earth Sciences, vol. 48(2), p. 183-192. https://doi.org/10.1046/j.1440-0952.2001.00854.x

Michaelsen, P., Henderson, R.A. 2000a. Facies relationships and cyclicity of high-latitude, Late Permian coal measures, Bowen Basin, Australia. International Journal of Coal Geology, vol. 44(1), p. 19-48. https://doi.org/10.1016/S0166-5162(99)00048-8

Michaelsen, P., Henderson, R.A. 2000b. Sandstone petrofacies expressions of multiphase basinal tectonics and arc magmatism: Permian-Triassic north Bowen Basin, Australia. Sedimentary Geology, v. 136(1-2), p. 113-136. https://doi.org/10.1016/S0037-0738(00)00090-7

Michaelsen, P., Henderson, R.A., Crosdale, P.J., Mikkelsen, S.O. 2000. Facies architecture and depositional dynamics of the Upper Permian Rangal Coal Measures, Bowen Basin, Australia. Journal of Sedimentary Research, vol. 70(4), p. 879-895. https://doi.org/10.1306/2DC4093F-0E47-11D7-8643000102C1865D

Michaelsen, P., Foster, C.B., Henderson, R.A. 1999: Destabilization and collapse of a long-lived (c. 9 My) peat mire ecosystem and dramatic changes of alluvial architecture: Permian-Triassic boundary, northern Bowen Basin, Australia. In: Yin, H., Tong, J. (eds.) International conference on Pangea and the Paleozoic-Mesozoic transition, Wuhan, China, 9-11 March, 1999, p. 137-140.

Miller, M.F., Curran, H.A., Martino R.L. 1998. Ophiomorpha Nodosa in estuarine sands of the lower Miocene Calvert Formation at the Pollack farm site, Delaware. Delaware Geological Survey Special Publication, vol. 21, p. 41-46.

Mironov, K.V. 1964. Geologiia mestorozhdenii uglia i goriuchikh slantsev SSSR, vol. 8, Moscow.

Nagy, J. Rodríguez Tovar, F.J., Reolid, M. 2016.

Environmental significance of Ophiomorpha in a transgressive-regressive sequence of the Spitsbergen Paleocene. Polar Research, vol. 35, 24192. https://doi.org/10.3402/polar.v35.24192

Naik, A.S., Behera, B., Shukla, U.K., Sahu, H.B., Singh, P.K., Mohanty, D., Sahoo, K., Chatterjee, D. 2021. Mineralogical Studies of Mahanadi Basin coals based on FTIR, XRD and Microscopy: A Geological Perspective. Journal of the Geological Society of India, vol. 97, p. 1019-1027. https://doi.org/10.1007/s12594-021-1817-9

Orolmaa, D., Uranbileg, L., Badarch, G. 1999. Stratigraphic questions of coal-bearing deposits in the vicinity of the spring Yamaan-Us bulag. Mongolian Geoscientist, vol. 14, p. 2-8.

Parihar, V.S., Nama, S.L., Khichi, C.P., Shekhawat, N.S., Snehlata, M., Mathur, S.C. 2016: Near Shore Shallow Marine (Ophiomorpha and Margaritichnus) Trace Fossils from Fatehgarh Formation of Barmer Basin, Western Rajasthan, India. Journal of Ecosystem & Ecography, vol. 6, 180. https://doi.org/10.4172/2157-7625.1000180

Pemberton, S.G., Frey, R.W. 1982. Trace fossil nomenclature and the Planolites-Palaeophycus dilemma. Journal of Paleontology, vol. 56(4), p. 843-881. https://www.jstor.org/stable/1304706

Postma, G., Nemec, W. 1990. Regressive and transgressive sequences in a raised Holocene gravelly beach, southwestern Crete. Sedimentology, vol. 37(5), p. 907-920. https://doi.org/10.1111/j.1365-3091.1990.tb01833.x

Rampino, M.R., Prokoph, A., Adler, A. 2000. Tempo of the end-Permian event: High-resolution cyclostratigraphy at the Permian-Triassic boundary. Geology, vol. 28(7), p. 643-646. https://doi.org/10.1130/0091-7613(2000)028<0643:TOTEPE>2.3.CO;2

Reading, H.G., Collinson, J.D. 1996. Clastic Coasts. In: Reading, H.G. (ed.) Sedimentary Environments: Processes, Facies and Stratigraphy. Third Edition. Blackwell Science, p. 154-231.

Reineck, H.E., Singh, I.B. 1980. Depositional Sedimentary Environments, Second Edition. Springer Verlag, Berlin, 551 p. https://doi.org/10.1007/978-3-642-81498-3

Retallack, G.J. 2013. Permian and Triassic greenhouse crises. Gondwana Research, vol. 24(1), p. 90-103. https://doi.org/10.1016/j.gr.2012.03.003

Ross, C.A., Ross, J.R.P. 1994: Permian sequence stratigraphy and fossil zonation. In: Embry, A.F., Beauchamp, Glass, D.J. (eds.) Pangea: Global Environments and Resources. Canadian Society of Petroleum Geologists Memoir, vol. 17, p. 219-231.

Saha, A., Chakrabarty, S., Bhattacharya, B. 2022. Evidence of the Permian marginal marine sedimentation recorded in sub-surface drill cores, Lower Gondwana successions, southern India. Journal of Earth System Science, vol. 131, 134. https://doi.org/10.1007/s12040-022-01866-5

Schachat, S.R., Labandeira, C.C., Gordon, J., Chaney, D., Levi, S., Halthore, M.N., Alvarez, J. 2014. Plant-Insect Interactions from Early Permian (Kungurian) Colwell Creek Pond, North-Central Texas: The Early Spread of Herbivory in Riparian Environments. International Journal of Plant Sciences, vol. 175(8), p. 855-890. https://doi.org/10.1086/677679

Schultz, B.P., Vickers, M.L., Huggett, J., Madsen, H., Heilmann-Clausen, C., Friis, H., Suess, E. 2020. Palaeogene glendonites from Denmark. Bulletin of the Geological Society of Denmark, vol. 68, p. 23-35. https://doi.org/10.37570/bgsd-2020-68-03

Schultz, B.P. 2009. Pseudomoroh after ikaite - called Glendonite is it a geological thermometer in cold sediments or geological oddity as it occurs close to PETM in the Fur formation. IOP Conference Series. Earth and Environmental Science, vol. 6, 072059. https://doi.org/10.1088/1755-1307/6/7/072059

Selleck, B.W., Carr, P.F., Jones, B.G. 2007. A review and synthesis of glendonites (pseudomorphs after ikaite) with new data: assessing applicability as recorders of ancient cold water conditions. Journal of Sedimentary Research, vol. 77, p. 980-991. https://doi.org/10.2110/jsr.2007.087

Simões, M.G., Matos S.A., Anelli, L.E., Rohn, R. Warren, L.V., David, L.M. 2015. A new

Permian bivalve-dominated assemblage in the Rio do Rasto Formation, Paraná Basin, Brazil: Faunal turnover driven by regional scale environmental changes in a vast epeiric sea. Journal of South American Earth Sciences, vol. 64(1), p. 14-26. https://doi.org/10.1016/j.jsames.2015.09.009

Smith, N.D. 1970. The Braided Stream Depositional Environment: Comparison of the Platte River with Some Silurian Clastic Rocks, North-Central Appalachians. Geological Society of America, Bulletin, vol. 81(10), p. 2993-3014. https://doi.org/10.1130/0016-7606(1970)81[2993:TBSDEC]2.0.CO;2

Storetvedt, K.M., Michaelsen, P. 2024. Sedimentary basins, hydrocarbons, graphite, coal, and Cu-Au deposits - from Mongolia to the Pacific margin: Interplay between the ubiquitous orthogonal fracture network and Global Wrench Tectonics. Mongolian Geoscientist, vol. 29 (58), p. 19-54.

Storetvedt, K.M. 2003. Global Wrench Tectonics. Bergen, Fagbokforlaget, 397 p.

Surlyk, F., Arndorff, L., Hamann, N.-E., Hamberg, L. Johannessen, P.N., Koppelhus, E.B., Nielsen, L.H., Noe-Nygaard, N., Pedersen, G.K., Petersen, H.I. 1995. High-resolution sequence stratigraphy of a Hettangian-Sinemurian paralic succession, Bornholm, Denmark. Sedimentology, vol. 42, p. 323-354. https://doi.org/10.1111/j.1365-3091.1995.tb02105.x

Tiwari, H.P., Halder, S.K., Das, A., Mishra, P., Kumar, A., Khattri, P. 2017. Potential Use of High Ash Indian Medium Coking Coal in Stamp Charged Coke Making. International Journal of Coal Preparation and Utilization, vol. 39(2), p. 101-111. https://doi.org/10.1080/19392699.2017.1305959

Uchman, A. 1995. Taxonomy and palaeoecology of flysch trace fossils: The Marnoso-arenacea Formation and associated facies (Miocene, Northern Apennines, Italy). Beringeria, v. 15, p. 3.

Weisenfluh, G.A., Ferm, J.C. 1984, Geologic controls on deposition of the Pratt seam, Black Warrior Basin, Alabama, U.S.A. In: Rahmani, R.A., Flores, R.M. (eds.) Sedimentology of Coal and Coal-bearing Sequences, International Association of Sedimentologists, Special Publication 7, p. 317-330. https://doi.org/10.1002/9781444303797.ch18

Wu, C., Kim, W., Herring, R., Cardenas, B.T., Dong, T.Y., Ma, H., Moodie, A., Nittrouer, J.A., Tsai, F., Li, A. 2023. Lowland river sinuosity on Earth and Mars set by the pace of meandering and avulsion. Nature Geoscience, vol. 16, p. 747-753. https://doi.org/10.1038/s41561-023-01231-1

Yin, H., Zhang, K., Tong, J., Yang, Z., Wu, S. 2001. The Global Stratotype Section and Point (GSSP) of the Permo-Triassic boundary. Episodes, vol. 24(2), p. 102-114. https://doi.org/10.18814/epiiugs/2001/v24i2/004